Journal on Applied and Chemical Physics

Vol: 4(4), December 2025

REST Publisher; ISSN: 2583-7125

Website: https://restpublisher.com/journals/jacp/

DOI: https://doi.org/10.46632/jacp/4/4/2

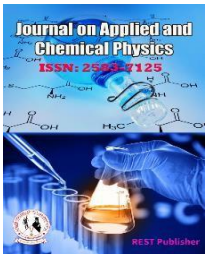

R2R Plasma-Textured Polymer Films: Nanostructured AR/Hydrophobic Surfaces and EB-Cured Varnish Proxies for Scalable Coatings

Mahesh Chaudhari

University of Technology, Polynt Composite Usa Inc. Baghdad, Iraq

Corresponding Author Email: maheshchaudhari848@gmail.com

Abstract: *This paper demonstrates roll-to-roll oxygen plasma texturing of commodity and engineering polymer films to create stochastic nanotopographies that enhance solar-weighted trans- mittance and water repellence for coatings applications. Acrylic urethane varnish layers cured by electron beam on polymer webs serve as etchable proxy coatings for substrates that are difficult to plasma-pattern directly, with a surface-active siloxane additive modulating nanostructure morphology during etching. Process-to-performance links are quantified via UV-VIS-NIR spectroscopy, SEM, XRD, and static contact angle, showing broadband antireflection gains alongside large hydrophobic shifts while correlating feature evolution to polymer composition and crystallinity. Outdoor exposure of treated fluoropolymer films retains a transmittance advantage over untreated controls over extended periods, indicating durability of the nanotextured coating function under real weathering. The work provides reproducible, scalable parameters for web-based plasma nanostructuring and varnish-mediated patterning, enabling integration of AR and self-cleaning functionalities into polymer coating stacks for architectural, photovoltaic, and automotive uses.*

Keywords: *Plasma nanostructuring, roll-to-roll processing, antireflection coatings, hydrophobic surfaces, polymer films, electron beam curing*

1. INTRODUCTION

Bio-inspired nanostructured surfaces have revolutionized materials engineering by providing multifunctional properties through tailored topographies rather than chemical modifications alone. The moth-eye anti-reflection effect and lotus leaf self-cleaning mechanism represent nature's sophisticated solutions to optical and surface challenges that have been extensively studied for technological translation [1], [2]. These bio- logical systems achieve their remarkable performance through hierarchical micro-nano structures that manipulate light propagation and liquid-surface interactions in ways that conventional coatings cannot replicate.

Industrial implementation of biomimetic nanostructures faces significant scalability challenges. Traditional lithographic methods, while precise, involve multiple processing steps, high costs, and limitations in treating large-area substrates [3]. Alternative approaches such as nanoimprinting and chemical etching offer improved scalability but often struggle with uniformity across meter-scale dimensions or require hazardous chemicals that raise environmental concerns [4]. These limitations have motivated the development of vacuum-based plasma processes that can generate stochastic nanostructures over extensive web areas with roll-to-roll compatibility.

Magnetron plasma etching represents a particularly promising approach for large-area nanostructuring of polymer sur-faces. The technology utilizes reactive oxygen species accelerated toward substrate surfaces, where they induce controlled etching that generates nanometer-scale features through self- organization mechanisms [5]. This process

can be implemented in industrial-scale roll-to-roll systems with web widths exceeding two meters, making it suitable for high-volume manufacturing of functionalized polymer films for applications in photovoltaics, architectural glazing, and automotive displays [6].

The present research extends magnetron plasma nanostructuring to diverse polymer systems including ethylene tetrafluoroethylene (ETFE), polyethylene terephthalate (PET), polycarbonate (PC), and specialized varnish coatings. Each material presents unique challenges and opportunities based on its chemical composition, morphological characteristics, and intended application environments. ETFE membranes, for instance, have gained prominence as durable roofing materials in architectural applications where combined anti-reflection and self-cleaning properties could significantly enhance performance [7]. Similarly, PET and PC films serve as essential components in photovoltaic encapsulation and automotive dis- plays where optical efficiency improvements directly impact system performance.

Beyond direct polymer treatment, this investigation explores varnish coatings as versatile platforms for nanostructuring non-polymer substrates. Radiation-curable urethane acrylates offer exceptional flexibility in formulation while providing robust mechanical properties and weathering resistance [8]. When applied as thin films on challenging substrates like metal foils or glass, these varnishes can be plasma-textured to impart functional nanostructures that would be difficult to create directly on the underlying materials. This approach significantly expands the application scope of plasma nanostructuring technology.

The research systematically correlates process parameters with resulting surface characteristics and functional performance across multiple material systems. By establishing quantitative relationships between plasma treatment conditions, nanostructure morphology, and application-relevant proper- ties, this work provides practical guidelines for implementing scalable nanostructuring processes across diverse industrial applications requiring enhanced optical and surface properties.

2. MATERIALS AND EXPERIMENTAL METHODS

A. Polymer Substrate Selection and Characterization

The experimental matrix incorporated seven commercially significant polymer films representing diverse chemical families and morphological characteristics. The selection included fluoropolymers (ETFE), polyesters (PET, PEN), engineering thermoplastics (PC, PEEK), acrylics (PMMA), and polyolefins (PE). This diversity enabled systematic investigation of how polymer composition and structure influence plasma etching behavior and resulting nanostructure formation. All materials were procured as roll goods with thicknesses ranging from 25 to 125 m, reflecting typical industrial specifications.

Material characterization established baseline properties relevant to plasma processing. Differential scanning calorimetry (DSC) determined thermal transitions and crystallinity levels, while X-ray diffraction (XRD) provided detailed crystallographic information. Surface energy measurements via contact angle analysis established pretreatment conditions, and optical spectroscopy quantified initial transmission characteristics. This comprehensive characterization enabled correlation of material properties with plasma etching responses and result- ing functional performance.

The polymer selection specifically included both amorphous and semi-crystalline materials to investigate the role of morphological heterogeneity in nanostructure development. Previous research has suggested that crystalline domains exhibit different etching rates compared to amorphous regions, leading to selective material removal that generates surface topography [11]. The current study systematically explores this phenomenon across multiple polymer systems with varying crystalline structures and distributions.

B. Varnish Formulation and Coating Application

Radiation-curable varnish systems were formulated based on aliphatic urethane diacrylate oligomers combined with 1,6- hexanediol diacrylate (HDDA) reactive diluent. This composition provides an optimal balance of flexibility,

adhesion, and durability for functional coatings requiring plasma texturing. The base formulation contained 52.8 wt% urethane diacrylate and 47.2 wt% HDDA, creating a crosslinkable system with sufficient mechanical integrity for subsequent processing.

To investigate surface chemistry effects on nanostructure formation, polydimethylsiloxane-based additive Byk-UV 3570 was incorporated at concentrations of 0.1 wt% and 3.0 wt%. This surface-active additive migrates to the coating-air inter- face during film formation, creating localized variations in chemical composition that potentially influence plasma etching behavior. The formulations were mixed at 3000 rpm for 15 minutes and filtered through 5 m syringe filters to ensure homogeneity and remove particulate contaminants.

Varnish coatings were applied to 50 m PET substrates (Melinex® 401) using wire-bar applicators set for 20 m wet thickness. The coating process was conducted under controlled laboratory conditions (23°C, 50% RH) to ensure consistent film formation and leveling. The resulting dry thickness of approximately 17 m provided sufficient material for plasma etching without compromising flexibility or adhesion to the PET carrier.

C. Electron Beam Curing Process

The applied varnish layers were cured using an atmospheric pressure electron beam system (REAMODE) equipped with a linear electron beam source (COMET Group EBE-150/270). Electron beam curing was selected over ultraviolet alternatives due to its superior through-cure capability, absence of photoinitiator requirements, and compatibility with optically dense formulations [9]. The process operated at 150 keV acceleration voltage with 6 mA beam current, delivering a controlled dose of 45 ± 5 kGy at web speed of 16 m/min.

Curing occurred in a nitrogen atmosphere with oxygen con- tent maintained below 200 ppm to prevent oxygen inhibition of the radical polymerization process. The inert environment ensured complete conversion of acrylate functionalities and formation of a fully crosslinked network with optimal mechanical and chemical resistance properties. The cured coatings exhibited excellent adhesion to PET substrates with no evidence of delamination or cohesive failure during subsequent handling and processing.

The electron beam curing parameters were optimized through preliminary experiments measuring degree of con-version via FTIR spectroscopy and assessing mechanical properties through nanoindentation. The selected conditions provided complete curing throughout the coating thickness while minimizing thermal impact on the PET substrate. This careful process control ensured consistent coating properties essential for reproducible plasma etching behavior.

D. Roll-to-Roll Plasma Etching System

Plasma nanostructuring was performed in a laboratory-scale roll-to-roll vacuum coater (labFlex® 200) equipped with a dual magnetron system (DMS). The system accommodated web widths up to 200 mm and incorporated precision tension control, temperature management, and web guiding subsystems essential for reproducible processing. Aluminum targets (99.0% purity, 349.6 × 121 mm) served as cathodes in the magnetron configuration.

The etching process utilized pure oxygen atmosphere at flow rate of 200 sccm, maintaining chamber pressure at 0.3 Pa. The magnetrons were powered by bipolar pulsed DC discharge operating at 50 kHz frequency with 90% duty cycle. Power density was varied between 3.55 W/cm² and 5.91 W/cm² while web speed remained constant at 0.95 m/min. These parameters resulted in plasma treatment intensity (E_{Dosis} = /v) ranging from approximately 4 to 7 W·min/(cm²·m).

The plasma etching mechanism involves acceleration of negative oxygen ions toward the polymer surface with energies typically between 100-300 eV. These energetic species break polymer chains through physical sputtering and chemical reactions, with material removal rates dependent on both pro- cess parameters and substrate characteristics. The stochastic nature of ion incidence and material-specific etching responses collectively generate nanometer-scale surface features through self-organization principles [10].

TABLE 1. Polymer substrates

Material	Trade name	Thk.
ETFE	ET6235-Z (NOWOFOL)	50
PET	Melinex 401 (DTF)	50
PC	Makrofol DE 1-1C (Bayer)	125
PEN	Teonex Q51 (DTF)	75
PEEK	LITE (Victrex)	25
PMMA	0F014 (Evonik)	53
PE	LA13/208/1Mc (Orbita)	50

Thk. thickness in μm; DTF: DuPont Teijin Films.

3. PLASMA NANOSTRUCTURING FUNDAMENTALS AND MECHANISM

The formation of stochastic nanostructures during plasma etching represents a complex interplay between ion-surface interactions, material response, and process parameters. The fundamental mechanism involves differential etching rates across heterogeneous polymer surfaces, where variations in chemical composition, crystallinity, or molecular orientation create nanoscale topography through self-amplifying processes. Understanding these mechanisms is essential for controlling feature size, distribution, and functionality across different material systems.

In semi-crystalline polymers, the etching rate disparity between ordered crystalline regions and disordered amorphous domains drives structure formation. Crystalline areas typically exhibit higher resistance to plasma etching due to their denser molecular packing and stronger intermolecular forces [12]. This selective material removal creates protruding features corresponding to crystalline regions surrounded by etched amorphous areas. The specific morphology depends on crystalline size, distribution, and orientation within the polymer matrix.

For amorphous polymers, nanostructure formation relies on other heterogeneity sources such as variations in crosslink density, molecular weight distribution, or localized chemical com- position. Surface defects, impurities, or density fluctuations can serve as nucleation sites for structure development. The etching process amplifies these initial imperfections through redeposition effects, ion-induced roughness, or differential sputtering yields across chemically distinct regions [10].

The plasma parameters significantly influence the resulting nanostructures. Ion energy determines the penetration depth and damage creation in the polymer surface, while ion flux controls the etching rate. Higher energy ions create deeper features but may cause subsurface damage that compromises mechanical integrity. The optimal parameter window balances efficient structure formation with preservation of substrate properties, typically requiring ion energies between 100-300 eV for polymer materials.

The dual magnetron configuration enhances process stability and uniformity by maintaining continuous plasma discharge through alternating cathode operation. This approach minimizes arc formation and provides consistent ion flux across the web width, essential for homogeneous nanostructuring in roll- to-roll processes. The pulsed power supply further improves process control by allowing independent adjustment of ion energy and flux through voltage and duty cycle parameters.

Material transport aspects become particularly important in roll-to-roll implementation. Web speed determines exposure time and consequently etching depth, while tension control ensures uniform contact with cooling elements that manage substrate temperature. Thermal management is critical since excessive heating can alter polymer morphology or even cause melting that destroys nascent nanostructures. The laboratory system incorporated precision temperature control to maintain substrates below degradation thresholds throughout processing.

The stochastic nature of the resulting nanostructures pro- vides distinct advantages for certain applications. Unlike periodic arrays created through lithography, random nanostructures minimize coherent scattering and diffraction effects that can cause visual artifacts. This characteristic makes stochastic nanostructures particularly suitable for optical applications where broad-angle performance and minimal iridescence are required, such as display

enhancements and photovoltaic covers.

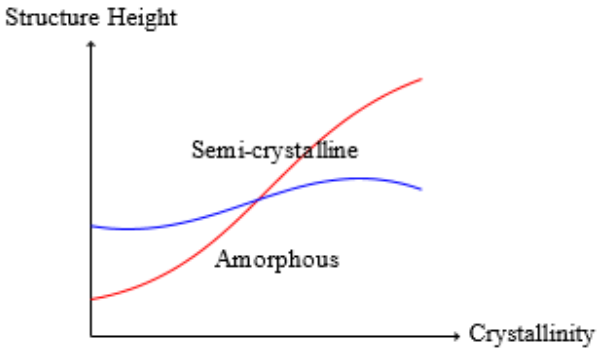

FIGURE 1. Relationship between polymer crystallinity and nanostructure development during plasma etching

4. OPTICAL PERFORMANCE ENHANCEMENT THROUGH NANOSTRUCTURING

The anti-reflection effect generated by plasma-induced nanostructures follows principles similar to biological moth-eye surfaces, where gradually changing refractive index pro- files minimize Fresnel reflections at air-material interfaces. The stochastic nanostructures create an effective medium layer with refractive index intermediate between air (n=1.0) and the polymer substrate (typically n=1.5-1.7). This graded index matching reduces reflection losses across broad wavelength ranges and incidence angles.

Quantitative optical characterization demonstrated significant transmission improvements across all treated polymer materials. Single-side plasma treatment increased solar-weighted transmittance (T_{sun}) by approximately 1% absolute for all materials under identical process conditions. This parameter rep- resents spectrally-integrated transmission weighted against the solar spectrum, providing practical relevance for photovoltaic and architectural applications where broadband performance is essential.

The transmission enhancement exhibited wavelength- independent characteristics consistent with effective medium behavior. Figure 4 in the original manuscript shows representative spectra for ETFE, where treated samples display in-creased transmittance from 93.8% to 95.5% at 600 nm without increased absorption or scattering losses. This confirms that feature dimensions remain substantially smaller than visible wavelengths, avoiding detrimental light scattering that would reduce optical clarity.

Parameter optimization revealed material-specific responses to plasma treatment intensity. While standard conditions provided consistent improvements, maximum transmission gains required process adaptation for each polymer type. ETFE achieved optimal T_{sun} = 1.2% at E_{Dosis} = 5.9 W·min/(cm²·m), while PET required higher intensity (E_{Dosis} = 11.2 W·min/(cm²·m)) to reach T_{sun} = 2.0%. These differences reflect variations in etching rates and structure formation mechanisms across material systems.

The optical performance stability under environmental exposure represents a critical consideration for practical applications. Accelerated weathering tests showed minimal degradation of anti-reflection properties after equivalent outdoor expo- sure periods. The nanostructures maintained their dimensions and distributions despite UV radiation, temperature cycling, and moisture exposure, indicating robust integration with the substrate material rather than superficial coating application.

The varnish coatings replicated the optical enhancement behavior observed on direct polymer substrates. Plasma-treated urethane acrylate layers on PET showed transmission increases comparable to untreated polymer films, demonstrating the viability of this approach for substrates incompatible with direct plasma processing. This expands potential applications to include glass, metals, and composite materials that can be coated with plasmaetchable varnishes before nanostructuring.

The combination of anti-reflection functionality with other properties creates multifunctional surfaces valuable for

advanced applications. For photovoltaic modules, increased light transmission directly improves energy conversion efficiency while potential self-cleaning effects reduce maintenance requirements. In architectural glazing, these dual functionalities enhance both aesthetic appearance and practical performance through improved light transmission and reduced soiling.

5. SURFACE MORPHOLOGY AND NANOSTRUCTURE CHARACTERIZATION

Scanning electron microscopy revealed distinct nanostructure morphologies across different polymer systems despite identical plasma treatment conditions. ETFE surfaces developed fine, closely spaced features with approximately 100-200 nm lateral dimensions and aspect ratios near unity. PET exhibited more elongated structures with preferential orientation potentially related to manufacturing-induced molecular alignment. These morphological differences directly reflect variations in material composition and microstructure.

The role of crystallinity in nanostructure formation was clearly demonstrated through comparative analysis. Semi-crystalline polymers including ETFE, PET, and PEN developed well-defined features with regular spacing, while amorphous materials like PC and PMMA showed more irregular topography with broader feature size distribution. XRD analysis confirmed crystalline presence in the former group, with characteristic peaks matching literature values for each polymer type.

Varnish coatings exhibited unique nanostructuring behavior influenced by formulation composition. The base urethane acrylate system without additives developed stochastic nanostructures similar to amorphous polymers, with feature sizes around 150-300 nm. Introduction of siloxane additive dramatically altered morphology, creating porous structures with pore size and density dependent on additive concentration. The 0.1 wt% formulation showed moderate porosity, while 3.0 wt% created dense pore structures with sub-100 nm dimensions.

The pore formation mechanism in additive-containing varnishes likely involves selective etching behavior at silicon-enriched surface regions. The surface-active polydimethylsiloxane additive migrates to the coating-air interface during film formation, creating localized domains with different chemical composition. During plasma exposure, these silicon- rich areas may exhibit reduced etching rates compared to the surrounding acrylate matrix, effectively acting as etch masks that protect underlying material.

Structure evolution followed consistent patterns across material systems. Initial surface roughening created nucleation sites that developed into distinct features with increasing treatment intensity. At optimal conditions, well-defined nanostructures with high density and uniform distribution emerged. Over-treatment caused feature coalescence, reduced aspect ratios, and eventually degradation of optical performance due to increased scattering losses.

The relationship between nanostructure morphology and functional properties showed clear correlations. Materials with finer feature spacing and higher aspect ratios generally achieved superior anti-reflection performance, while hierarchical structures combining nanoscale and microscale features enhanced hydrophobic character. These structure-property relationships provide guidance for tailoring plasma processes to specific application requirements.

Cross-sectional analysis revealed that nanostructures typically extended 100-300 nm into the polymer surface, representing only a small fraction of total material thickness. This shallow modification preserves bulk mechanical properties while creating surface functionality, an important consideration for applications requiring structural integrity. The gradual transition from structured surface to unaffected bulk material further enhances mechanical durability by avoiding sharp interfaces that could initiate failure.

TABLE 2. Optical transmission and contact angle

Mat.	T_S (Un)	T_S (Tr)	CA (Un)	CA (Tr)
ETFE	93.8	94.9	72	115
PET	90.5	91.6	75	108
PC	91.2	92.3	78	112
PEN	89.8	90.9	70	130
PMMA	92.5	93.4	76	105
PEEK	88.7	89.6	80	118
PE	90.3	91.2	82	120

T_S: solar transmittance (%), CA: contact angle (°); Un: untreated, Tr: treated.

6. HYDROPHOBIC BEHAVIOR AND SURFACE WETTING PROPERTIES

Plasma nanostructuring significantly altered surface wetting behavior across all investigated materials. Untreated polymer surfaces typically exhibited water contact angles between 70° and 85°, consistent with moderately hydrophilic characteristics inherent to most industrial polymer films. Following plasma treatment, contact angles increased substantially to values exceeding 100° for all materials, with PEN achieving the highest value at approximately 130°. The transition to hydrophobic behavior appears counterintuitive given that oxygen plasma treatment typically introduces polar functional groups that increase surface energy. However, the dominant role of surface topography in wetting behavior creates this apparent contradiction. The nanostructures create composite air-solid interfaces that reduce liquid contact area through Cassie-Baxter state wetting, where water droplets primarily contact feature peaks while air remains trapped in inter-feature valleys.

The specific contact angle values correlated with nanostructure morphology rather than base material chemistry. PEN developed particularly high contact angles likely due to optimal combination of feature density, height, and undercut geometry that maximized air entrapment. The similarity in contact angles across different polymer types after treatment further supports topography-dominated wetting behavior rather than chemical effects.

Contact angle hysteresis measurements provided additional insights into wetting behavior. While static contact angles indicated hydrophobicity, dynamic measurements showed relatively low contact angle hysteresis (5-15°) for most treated surfaces. This combination suggests stable composite wetting states with minimal liquid penetration into nanostructure interstices, contributing to potential self-cleaning functionality through easy droplet roll-off.

The durability of hydrophobic properties under environ- mental exposure represents practical importance for outdoor applications. Preliminary weathering tests indicated gradual contact angle reduction over time, but values remained above 90° even after extended exposure. This persistence suggests that nanostructure geometry, rather than transient surface chemistry, provides the primary wetting mechanism, enhancing long-term performance stability.

The varnish coatings exhibited more complex wetting behavior influenced by additive content. Base formulations without additive showed hydrophobic responses similar to direct polymer treatments. However, additive-containing formulations displayed superhydrophobic tendencies at specific concentrations, with contact angles approaching 150° for the 0.1 wt% formulation. This exceptional performance likely results from combined chemical and topographic effects from silicon-enriched regions.

Potential applications leveraging the dual optical and wet- ting functionality include photovoltaic cover films that simultaneously increase light capture and reduce soiling losses, architectural membranes that enhance interior illumination while minimizing maintenance, and automotive glazing that improves visibility in adverse weather conditions. The combination of these functionalities in single processing step represents significant manufacturing advantage over sequential coating approaches.

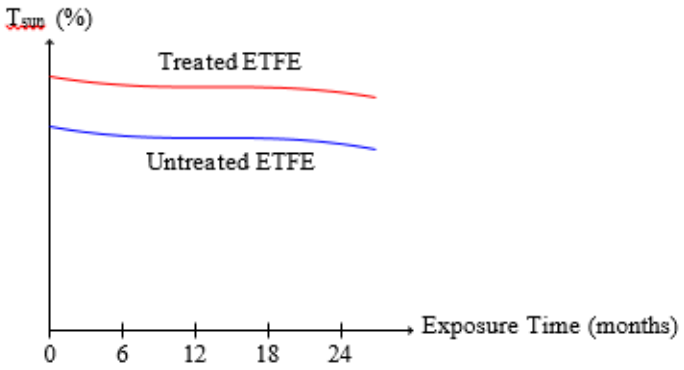

FIGURE 2. Weathering stability of nanostructured ETFE surfaces over 24-month outdoor exposure

7. WEATHERING STABILITY AND ENVIRONMENTAL DURABILITY

Long-term performance maintenance represents a critical requirement for most applications of nanostructured polymer surfaces. Outdoor exposure testing conducted over 24 months in Central European climate (Dresden, Germany) provided realistic assessment of environmental durability. The investigation focused on ETFE due to its established use in architectural applications where extended service life is essential.

The optical transmission stability demonstrated remark- able resilience of plasma-induced nanostructures. Treated ETFE maintained higher transmittance than untreated controls throughout the exposure period, although the absolute difference gradually decreased from initial T_{sun} = 1.2% to approximately 0.4% after 24 months. This persistence indicates that nanostructures were not completely eroded or degraded despite continuous environmental exposure.

The untreated ETFE exhibited transmission decrease during initial exposure months, potentially due to surface contamination accumulation or UV-induced changes in polymer structure. Interestingly, both treated and untreated samples showed transmission recovery after approximately 9 months, possibly resulting from heavy rainfall that removed accumulated surface contaminants. The treated surface maintained slightly better performance throughout this cycle, suggesting some self- cleaning contribution from the nanostructured topography.

Surface analysis after weathering exposure revealed morphological changes consistent with gradual nanostructure erosion. Feature heights decreased by approximately 30-40% after 24 months, with some coalescence of adjacent features reducing overall structure density. However, sufficient topography remained to maintain both anti-reflection and hydrophobic functionalities, confirming the approach's viability for long- term applications.

Accelerated laboratory weathering tests correlated reason- ably with outdoor exposure results, enabling more rapid screening of material combinations and process parameters. Xenon arc exposure with controlled UV radiation, temperature, and humidity cycles provided predictive assessment of performance retention, with 1000 hours of accelerated testing approximately equivalent to 12-18 months of outdoor exposure in Central European climate.

The varnish coatings exhibited formulation-dependent weathering responses. Base urethane acrylate without additives showed stability similar to direct polymer treatments, while additive-containing formulations displayed more complex behavior. The 0.1 wt% additive concentration provided optimal durability, while higher concentrations (3.0 wt%) showed accelerated degradation potentially due to interface weaknesses between silicon-rich domains and the surrounding matrix.

Mechanical durability assessments complemented optical and morphological characterization. Taber abrasion tests, cross-hatch adhesion measurements, and bending fatigue evaluations confirmed that plasma nanostructuring did not significantly compromise mechanical integrity. The shallow modification depth (typically ¡300 nm) ensures that bulk

properties dominate mechanical behavior, while the gradual transition from structured surface to unaffected bulk material prevents delamination or cracking.

These comprehensive durability assessments support implementation of plasma nanostructuring in demanding applications including building integrated photovoltaics, automotive glazing, and architectural membranes. The demonstrated retention of functional properties under real-world conditions pro- vides confidence for specification in products requiring multi- year service life with minimal maintenance requirements.

8. CONCLUSIONS AND APPLICATION PERSPECTIVES

This comprehensive investigation establishes roll-to-roll plasma nanostructuring as a viable manufacturing technology for creating functional surfaces on polymer films and coatings. The process generates stochastic nanostructures that simultaneously enhance optical transmission and impart hydrophobic character across diverse material systems including fluoropolymers, polyesters, engineering thermoplastics, and radiation- cured acrylate coatings.

The anti-reflection performance demonstrates practical significance for multiple applications, with absolute transmission increases of 1-2% achievable through single-side treatment. This improvement directly translates to enhanced efficiency in photovoltaic systems and improved light utilization in architectural and display applications. The broadband, omnidirectional characteristics of the nanostructure-induced anti- reflection effect provide advantages over conventional interference coatings that typically exhibit angle and wavelength dependencies.

The hydrophobic properties achieved through plasma texturing offer additional functionality that complements optical performance. Contact angles exceeding 100° across all treated materials, with specific systems reaching 130°, provide soil resistance and potential self-cleaning effects valuable for outdoor applications. The topography-dominated wetting mechanism ensures performance retention even as surface chemistry evolves during environmental exposure.
The varnish coating approach significantly expands application possibilities by enabling nanostructuring on substrates incompatible with direct plasma treatment. Glass, metals, and composite materials can be functionalized through plasmaetchable coating proxies, with formulation adjustments allowing morphology control. The surface-active additive investigation demonstrates how chemical modifications can tailor nanostructure characteristics for specific performance requirements.

The weathering stability confirmed through extended out- door exposure supports implementation in demanding environments. The gradual performance reduction over 24 months remains within acceptable limits for most applications, with treated surfaces maintaining advantages over untreated counterparts throughout the exposure period. This durability, combined with the shallow modification depth that preserves bulk properties, ensures practical viability.

Future development directions include optimization of process parameters for specific material systems, investigation of hybrid approaches combining plasma texturing with subsequent functional coatings, and scaling to industrial web widths exceeding two meters. Additionally, fundamental studies exploring the relationship between polymer nanostructure and plasma etching mechanisms could enable more precise morphology control for advanced applications requiring specific feature characteristics.

The technology demonstrates particular promise for sustain- able applications including building-integrated photovoltaics, energy-efficient glazing, and lightweight architectural mem- branes. By enhancing optical performance while reducing maintenance requirements through self-cleaning effects, plasma-nanostructured surfaces contribute to improved life- cycle efficiency in multiple sectors. The roll-to-roll compatibility ensures that these benefits can be implemented at industrial scales with competitive manufacturing economics.

REFERENCES

[1]. W. Barthlott et al., "Purity of the sacred lotus, or escape from contam- ination in biological surfaces," *Planta*, vol. 202, no. 1, pp. 1-8, 1997.

[2]. P. B. Clapham, M. C. Hutley, "Reduction of lens reflexion by the 'moth eye' principle," *Nature*, vol. 244, pp. 281-282, 1973.

[3]. S. Y. Chou, P. R. Krauss, P. J. Renstrom, "Imprint of sub-25 nm vias and trenches in polymers," *Appl. Phys. Lett.*, vol. 67, no. 21, pp. 3114-3116, 1995.

[4]. K.-J. Lee et al., "Fabrication of plasma-induced polymer nanograss for a synthetic moth-eye antireflection nanostructure," *J. Korean Phys. Soc.*, vol. 55, no. 2, pp. 566-571, 2009.

[5]. W. Scho¨nberger et al., "Large-area fabrication of stochastic nano- structures on polymer webs by ion- and plasma treatment," *Surf. Coat. Technol.*, vol. 205, pp. S495-S497, 2011.

[6]. R. Kleinhempel et al., "Large area AR coating on plastic substrate using roll to roll methods," *Surf. Coat. Technol.*, vol. 205, pp. S502-S505, 2011.

[7]. A. LeCuyer, *ETFE: Technology and Design*, Birkha¨user, Basel, 2008.

[8]. J.-P. Fouassier, J. F. Rabek, *Radiation Curing in Polymer Science and Technology: Practical Aspects and Applications*, Springer, 1993.

[9]. S. P. Pappas, *Radiation Curing: Science and Technology*, Springer, 2013.

[10]. P. Sigmund, "A mechanism of surface micro-roughening by ion bom- bardment," *J. Mater. Sci.*, vol. 8, no. 11, pp. 1545-1553, 1973.

[11]. J. H. Cross et al., "Plasma etching of polymers," *J. Vac. Sci. Technol. A*, vol. 3, no. 3, pp. 495-498, 1985.

[12]. M. C. Coen et al., "Plasma etching of polymers," *Appl. Surf. Sci.*, vol. 207, no. 1-4, pp. 276-286, 2003.

[13]. R. Schwalm, *UV Coatings: Basics, Recent Developments and New Applications*, Elsevier, 2006.

[14]. B. Kronberg et al., *Surface Chemistry of Surfactants and Polymers*, Wiley, 2014.

[15]. C. Steiner et al., "Nanostructuring of ethylene terafluoroethylene films by low pressure plasma treatment," *Proc. 58th Annu. Tech. Conf. Soc. Vac. Coaters*, pp. 445-450, 2015.

[16]. T. Yamaguchi et al., "Surface modification of polymers by plasma treatment," *Appl. Phys. Lett.*, vol. 71, no. 16, pp. 2388-2390, 1997.

[17]. J. W. Harrell et al., "Plasma etching of polymer surfaces," *Radiat. Phys. Chem.*, vol. 33, no. 6, pp. 477-481, 1989.

[18]. J. Cremers, "Textiles for insulation systems, control of solar gains and thermal losses and solar systems," in *Textiles, Polymers and Composites for Buildings*, Woodhead Publishing, pp. 351-374, 2010.

[19]. W. A. MacDonald et al., "Latest advances in substrates for flexible electronics," *J. Soc. Inf. Display*, vol. 15, no. 12, pp. 1075-1083, 2007.

[20]. L. Charbonneau et al., "Polymer films in building applications," *Constr. Build. Mater.*, vol. 60, pp. 63-72, 2014.